Moving Surface Boundary-Layer Control: Studies with Bluff Bodies and Application

V. J. Modi* and M. S. U. K. Fernando†
University of British Columbia, Vancouver, British Columbia, V6T 1W5 Canada
and
T. Yokomizo‡
Kanto Gakuin University, Mutsuura, Kanazawa, 236 Japan

The concept of moving surface boundary-layer control has proved quite successful in increasing lift and delaying stall of slender bodies like airfoil sections. This paper assesses effectiveness of the concept in reducing drag of bluff bodies, such as a two-dimensional flat plate at large angles of attack, rectangular prisms, and three-dimensional models of trucks, through an extensive wind-tunnel test program. Results suggest that injection of momentum through moving surfaces, achieved here by introduction of bearing mounted, motor-driven, hollow cylinders, can significantly delay separation of the boundary layer and reduce the pressure drag. A flow-visualization study, conducted in a closed-circuit water tunnel using slit lighting and polyvinylchloride tracer particles, complements the wind-tunnel tests. It shows, rather dramatically, effectiveness of the moving surface boundary-layer control.

Introduction

EVER since the introduction of the boundary-layer concept by Prandtl, there has been a constant challenge faced by scientists and engineers to minimize its adverse effects and control it to advantage. Methods such as suction, blowing, vortex generators, turbulence promoters, etc., have been investigated at length and employed in practice with a varying degree of success. A vast body of literature accumulated over years has been reviewed rather effectively by several authors including Goldstein,[1] Lachmann,[2] Rosenhead,[3] Schlichting,[4] Chang,[5] and others. However, the use of moving wall for boundary-layer control has received relatively less attention.

Irrespective of the method used, the main objective of a control procedure is to prevent or at least delay the separation of boundary-layer from the wall. A moving surface attempts to accomplish this in two ways:

1) It retards growth of the boundary-layer by minimizing relative motion between the surface and the free stream.

2) It injects momentum into the existing boundary-layer.

A practical application of moving wall for boundary-layer control was demonstrated by Favre.[6] Using an airfoil with upper surface formed by a belt moving over two rollers, he was able to delay separation until the angle of attack reached 55 deg where the maximum lift coefficient of 3.5 was realized. Alvarez-Calderon and Arnold[7] carried out tests on a rotating cylinder flap to develop a high-lift airfoil for STOL-type aircraft. The system was flight tested on a single engine high-wing research aircraft.

Of some interest is the North American Rockwell-designed OV-10A aircraft which was flight tested by NASA's Ames Research Center.[8-10] Cylinders located at the leading edges of the flaps were rotated at high speed with the flaps in lowered position. The main objective of the test program was to assess handling qualities of the propeller-powered STOL-type aircraft at higher life coefficients. The aircraft was flown at speeds of 29–31 m/s, along approaches up to −8 deg, which corresponded to a lift coefficient of about 4.3. In the pilot's opinion any further reductions in approach speed were limited by the lateral-directional stability and control characteristics.

In terms of trying to understand the phenomenon at the fundamental level, Tennant's contribution to the field is significant. Tennant et al.[11] have conducted tests with a wedge-shaped flap having a rotating cylinder as the leading edge. Flap deflection was limited to 15 deg and the critical cylinder velocity necessary to suppress separation was determined. Effect of increasing the gap size (between the cylinder and the flap surface) was also assessed. No effort was made to observe the influence of an increase in the ratio of cylinder surface speed (U_c) to the freestream velocity (U) beyond 1.2.

Through a comprehensive wind-tunnel test program involving a family of airfoils with one or more cylinders forming moving surfaces (Fig. 1), complemented by the surface singularity numerical approach and flow visualization, earlier studies by the authors have shown spectacular effectiveness of the concept, which increased the maximum life coefficient by more than 200% and delayed the stall angle to 48 deg[12,13] (Figs. 2 and 3).

The present study builds on this background and explores application of the concept of moving surface boundary-layer control to ground-based systems for drag reduction. The extensive wind-tunnel test program followed by a flow-visualization study investigates 1) a two-dimensional flat plate, with a rotating cylinder at each edge, in the subcritical range of the Reynolds number and the angle of attack, α, varying from 0 to 90 deg; 2) a family of two-dimensional rectangular prisms with rotating cylinders at two edges; and 3) a tractor-trailer configuration of the truck with the moving surface boundary-layer control applied at the top leading and trailing edges of the trailer.

A schematic diagram of the configurations studied is presented in Fig. 4. An important parameter in the study is the ratio of the cylinder surface velocity (U_c) to the freestream velocity (U), which was systematically varied during the test program conducted in the smooth flow condition.

Presented as Paper 90-0298 at the AIAA 28th Aerospace Sciences Meeting, Reno, NV, Jan. 8–11, 1990; received Feb. 16, 1990; revision received Feb. 19, 1991; accepted for publication Feb. 19, 1991.

*Professor. Fellow AIAA.

†Post-Doctoral Fellow, Department of Mechanical Engineering; currently at VIPAC Engineers & Scientists Ltd., Port Melbourne, Australia.

‡Professor, Department of Mechanical Engineering.

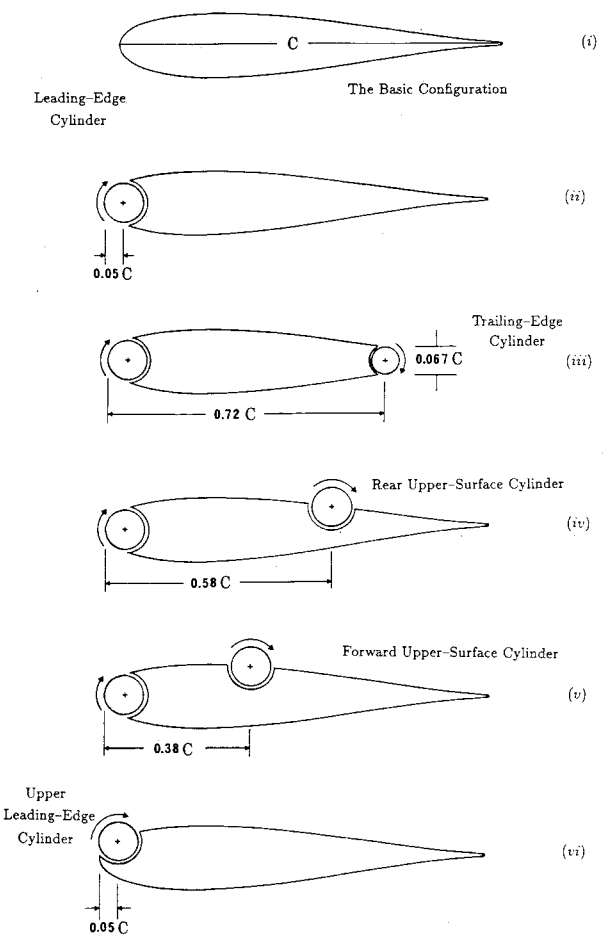

Fig. 1 Various rotating cylinder configurations used in earlier studies by the authors to increase lift and delay stall.[12,13]

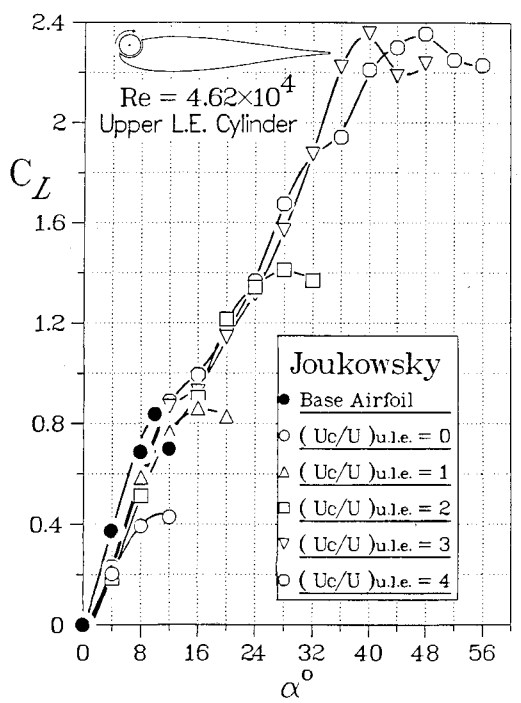

Fig. 2 Lift and stall characteristics of the Joukowsky model as affected by the upper leading edge cylinder rotation. The base airfoil data serve as reference to assess the effect of airfoil modification by the cylinder and its rotation.

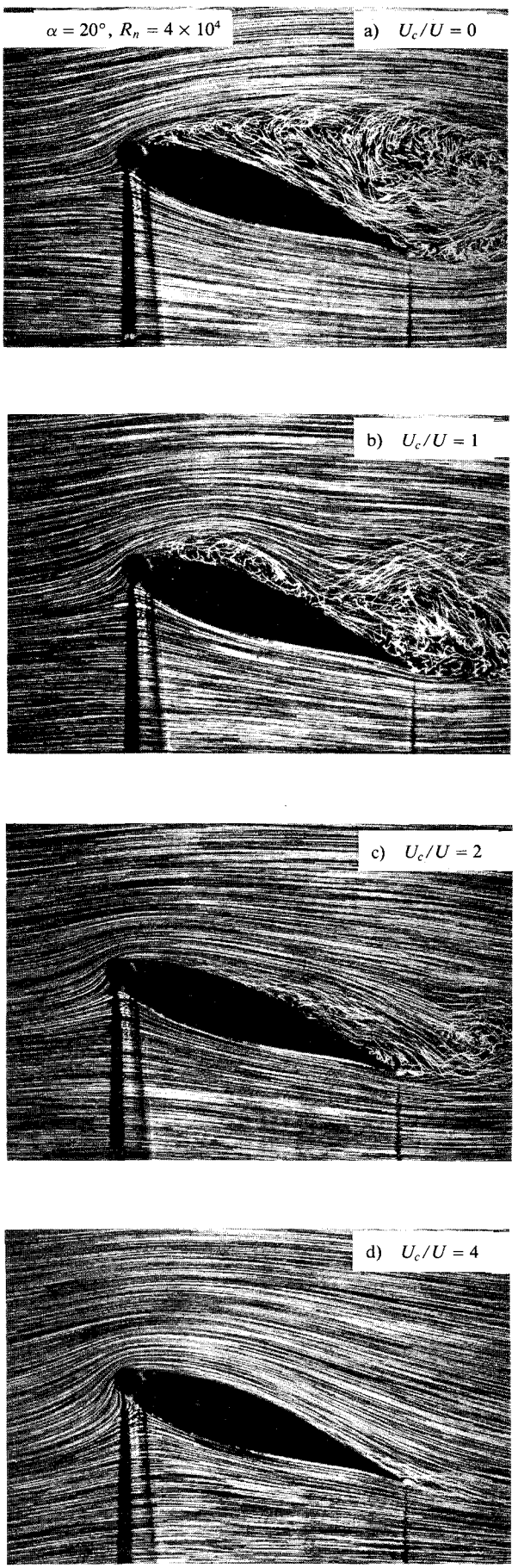

Fig. 3 Flow-visualization photographs showing the transition from a highly separated flow in absence of cylinder rotation to the essentially reattached flow at $U_c/U = 4$.

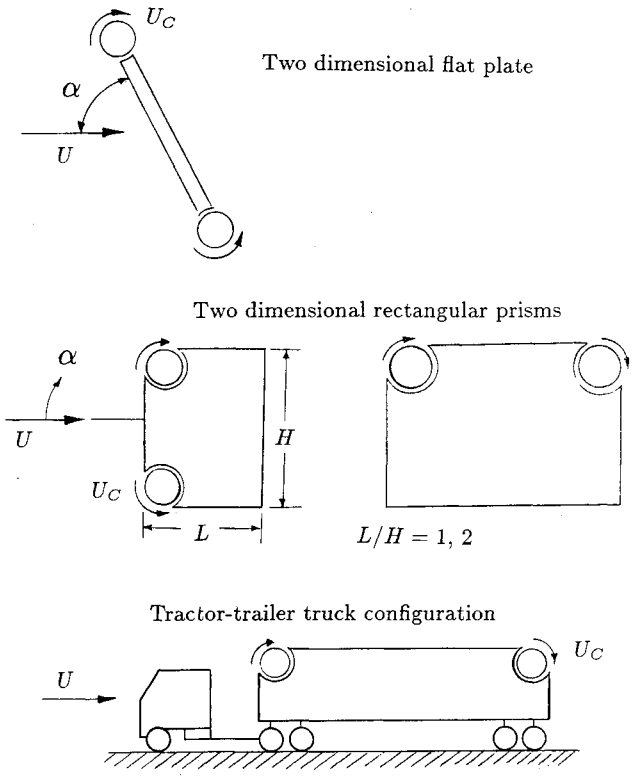

Fig. 4 Schematic diagrams of the bluff bodies studied during the wind-tunnel test program.

Models and Wind-Tunnel Test Program

Flat Plate and Rectangular Prisms

Two-dimensional flat plate and rectangular prisms were tested in a 45 × 45 cm cross-section wind tunnel with a maximum speed of 50 m/s. The large converging nozzle at the entrance of the tunnel (contraction ratio = 10:1) made the flow in the test section uniform with a level of turbulence less than 0.5%. The tunnel speed was adjusted by a variac transformer and measured using a pitot static tube connected to an inclined alcohol manometer.

A flat plate model, 9 × 40.5 cm, and two rectangular prism models with a span (B) of 40.5 cm and depth (L) to width (H) ratio L/H = 1,2 were constructed from Plexiglas. The models were equipped with two moving surface boundary-layer control elements (rotating cylinders) as shown in Fig. 4. The cylinders were driven by variac-controlled AC motors through flexible belt drives. The motor speed was monitored using a strobe light. In the present test program the ratio U_c/U was varied from 0 to 3. This corresponded to a maximum cylinder speed of around 11,000 rpm at a freestream speed of 5 m/s. To ensure two-dimensionality of the flow, the models were fitted with end plates. In general, the tunnel speed was kept constant at 5 m/s, which corresponds to a Reynolds number of 3 × 10^4 based on the freestream velocity and the model width (H). The lift and drag forces as well as pressure data were recorded over a range of the angle of attack at 5-deg increments. The force could be measured with an accuracy of 0.5 g/mV.

Tractor-Trailer Truck Configuration

A 1/12 scale model of a truck with leading and trailing edge cylinders on the trailer (Fig. 4) was tested in the boundary-layer wind tunnel at the University of British Columbia. The partial return-type tunnel has a test section 2.44 m wide and 24.4 m long, consisting of eight 3.05-m-long bays, and a variable height roof to allow for the boundary-layer correction. The present experiment was carried out in the first bay which provided smooth flow with a turbulence level less than 0.4%. The tunnel provides a stable wind speed in the range 2.5–25 m/s.

The model, supported using four steel guy wires attached to the tunnel roof, rested on cylindrical roller bearings, which restricted the lateral movement of the model while allowing for streamwise displacement. By appropriately adjusting the guy wire tension, the frictional contact forces on the model due to bearings were minimized. In general, the guy wires carried over 98% of the model weight leading to a minimal friction force, thus permitting accurate measurement of the drag. The sensitivity of the drag measurement in this case was around 0.4 g/mV.

Results and Discussion

Flat Plate

Figure 5 shows variation of the lift and drag coefficients (C_L, C_D) with the angle of attack at four different speed ratio (U_c/U = 0, 1, 2, 3) of the upstream (upper) cylinder when the downstream cylinder is at rest. With both the cylinders at rest, the plate stalls at around 10 deg (Fig. 5a); however, with the upstream cylinder rotation, the stall is delayed and there is a substantial increase in lift. The $C_{L,max}$ of 2.7 at U_c/U = 3 represents an increase of 200% compared to the nonrotating cylinder case. However, the focus here is on the drag, which for α = 90 deg and U_c/U = 3 corresponds to C_D = 1.1, a reduction of around 40% (Fig. 5b, C_D = 1.85 at U_c/U = 0).

Of course, the maximum reduction in wake and hence the corresponding decrease in the drag coefficient can be expected when both the cylinders are rotating as shown in Fig. 6. For α = 90 deg, a decrease in the drag coefficient from 1.85 at U_c/U = 0 to 0.47 at U_c/U = 3 represents a reduction of around 75%! The flow-visualization photographs also showed a re-

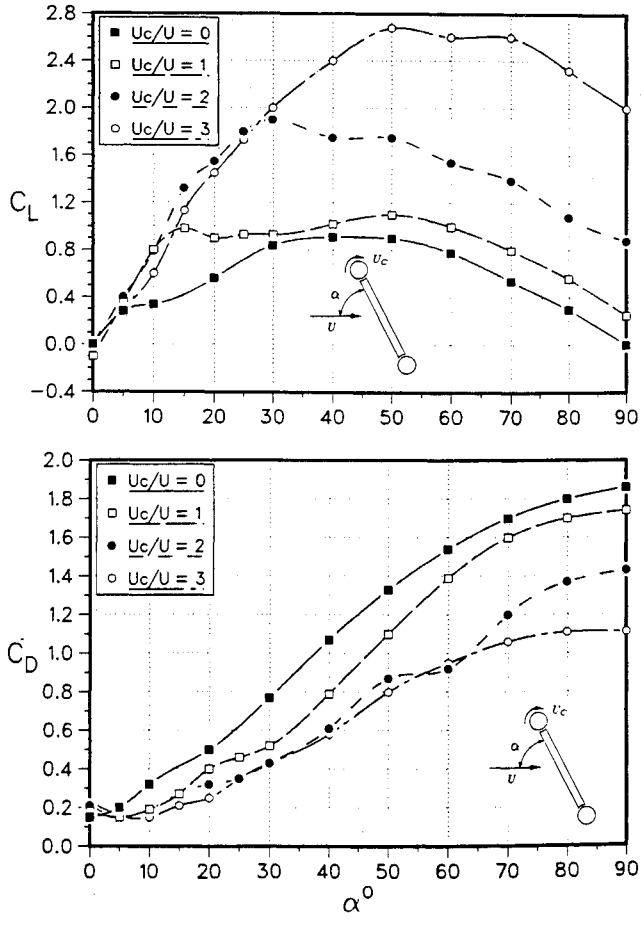

Fig. 5 Variation of the lift and drag coefficients for a two-dimensional flat plate when the moving surface boundary-layer control is applied at the upstream edge.

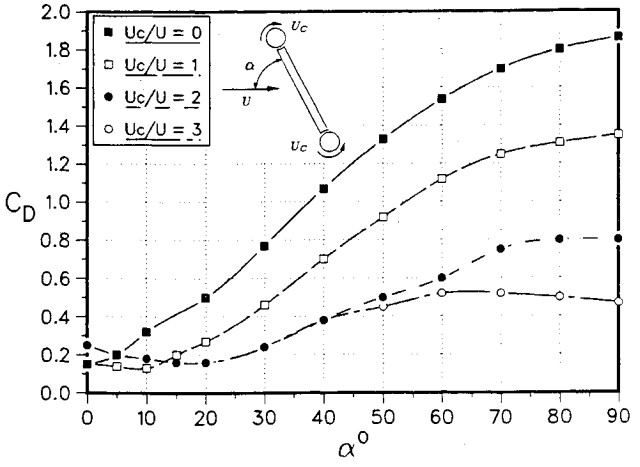

Fig. 6 Plots showing significant reduction in drag of a two-dimensional flat plate with the moving surface boundary-layer control applied at both the leading and trailing edges. Note, at α = 90 deg, a reduction in C_D is around 75%.

markable reduction in wake width, thus qualitatively substantiating the trend suggested by the wind-tunnel test results (Fig. 7).

Rectangular Prisms

Rectangular prisms with rotating cylinders at two adjacent corners provide three basic configurations for study: the side with cylinders facing the flow, forming the top face, or representing the rear face. Various intermediate configurations can be obtained by systematically changing the angle of attack. With two values of L/H to help assess the effect of boundary-layer reattachment and reseparation further downstream, and four values of U_c/U, the amount of information obtained is rather extensive. Only a few of the typical results useful in discerning trends are presented here.

Figure 8 presents results on variation of the drag coefficient with the angle of attack and cylinder rotation for prisms with square (L/H = 1) and rectangular (L/H = 2) cross sections. Note, for α = 0, the face with cylinders is normal to the freestream. For the square section prism (Fig. 8a), in absence of the cylinder rotation, the drag coefficient diminishes with an increase in the angle of attack in the range α = 0–10 deg. The drag coefficient is an integrated effect of the projected area normal to the flow as well as the effective wake width. At lower angles of attack (α ≤ 10 deg), although the projected area increases, the separating flow from the upstream nonrotating cylinder reattaches on the bottom face leading to an overall decrease in the drag coefficient. However, for α > 10 deg, the projected area continues to increase while the flow at the bottom face becomes progressively separated resulting in an increase in C_D. For the rectangular prism (L/H = 2, Fig. 8b), C_D increases with α over the entire range (α = 0–25 deg). This is understandable as now an increase in the projected area is sufficiently large to dominate any drag reduction caused by the reattachment of the boundary layer on the bottom face even at a small α. U_c/U = 0 plot serves as a reference to assess effect of the cylinder rotation.

With the rotation of the cylinders, the boundary-layer separation on the surface of the square prism is delayed, resulting in a relatively narrow wake and hence a reduction in the drag coefficient. At α = 0 deg and U_c/U = 3, the reduction in C_D was around 53%, and decreased to around 40% at α = 25 deg (Fig. 8a). The rectangular prism (Fig. 8b) showed essentially similar trend with an increase in U_c/U and gave a reduction in C_D for U_c/U = 3 of 38% at α = 0 deg (33% at α = 25 deg). Longer depth of the prism cross section makes the boundary-layer control only partly successful and the

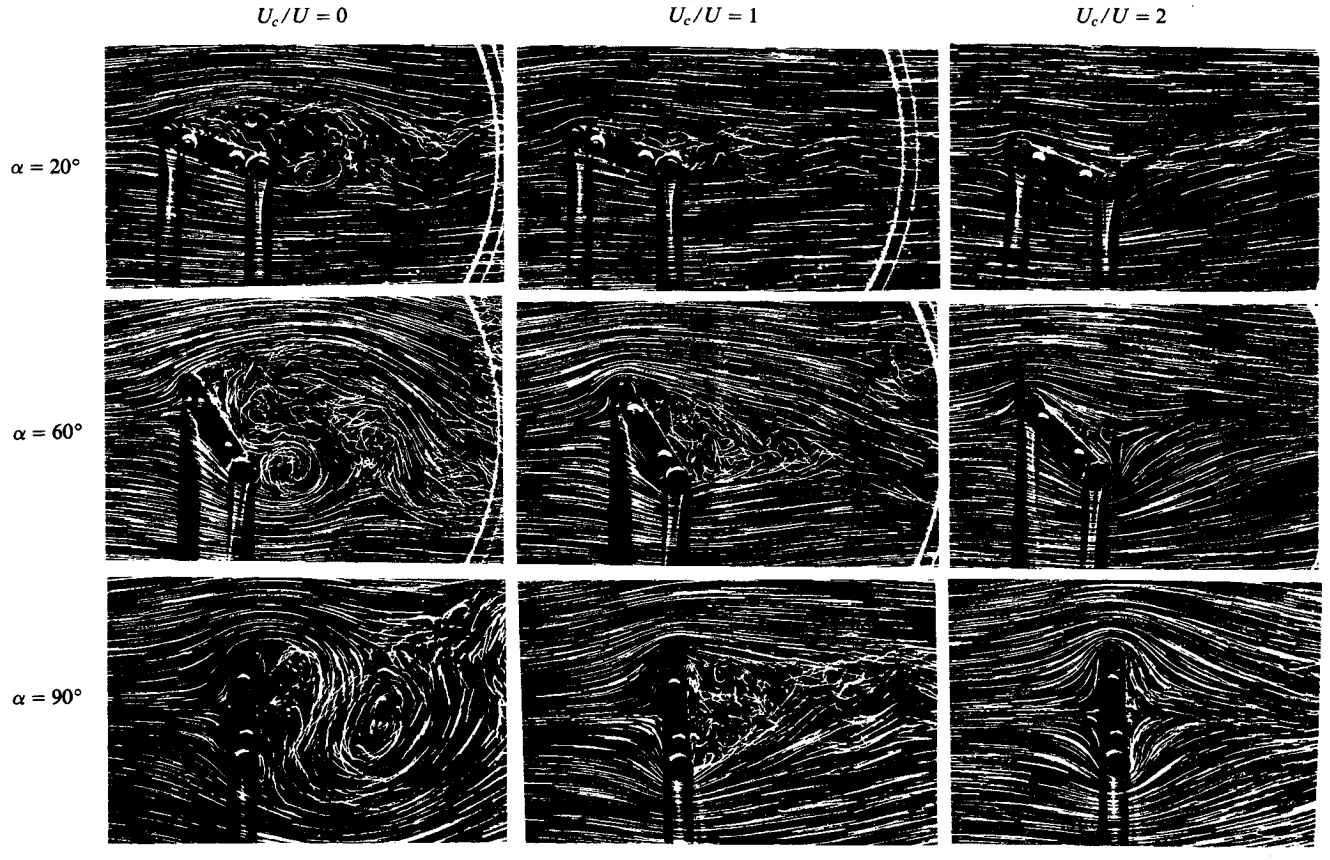

Fig. 7 Typical flow-visualization photographs for a flat plate at α = 90 deg showing dramatically effectiveness of the moving surface boundary-layer control applied at the top and bottom edges.

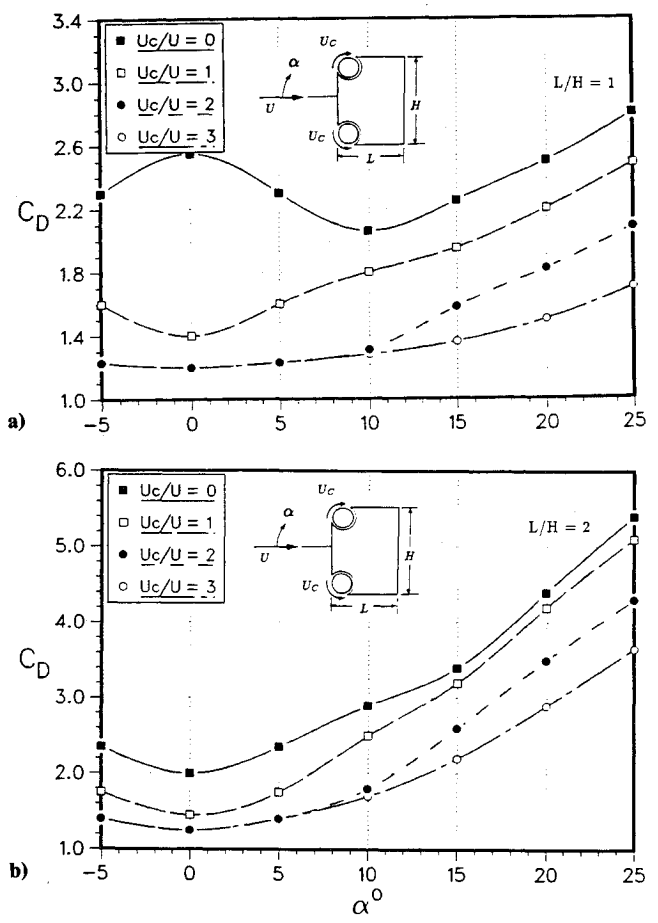

Fig. 8 Effect of the front face moving surface boundary-layer control on the variation of C_D vs α for two-dimensional prisms: a) $L/H = 1$; b) $L/H = 2$.

boundary layer separates before reaching the trailing edge. Note, with both the cylinders rotating the flow field is symmetrical, i.e., it is the same for a given positive or negative α. The plots in the range -5 deg $< \alpha < 5$ deg indicate this trend.

Figure 9 shows a sample of the representative results for the experimental phase where the rotating elements are on the top surface, i.e., on the face parallel to the freestream for $\alpha = 0$. Cases corresponding to single- and two-cylinder rotation for the square prism model are considered. At the outset it is apparent that rotation of the second cylinder has very little effect on the flow field, and hence on C_D, for $\alpha >$ 5 deg as now the trailing edge cylinder lies in the wake. However, for smaller and negative α, it is quite successful in further reducing C_D, from 1.7 at $\alpha = 0$ deg and $U_c/U = 3$ for the upstream cylinder rotation to 1.3 when both the cylinders are rotating. A reduction in the drag coefficient by 54% with both the cylinders rotating is indeed quite impressive.

The influence of rotating cylinders located on the rear vertical face of the square and rectangular prisms was also investigated. In this case, the boundary layer separates at the top and bottom leading edges and the rotating cylinders are submerged in the wake, thus reducing their effectiveness. Now the reduction in C_D at $\alpha = 0$ deg and $U_c/U = 3$ was found to be only 13% for the square prism and virtually zero for the rectangular prism (Fig. 10) compared to 53% and 40%, respectively, for the case with cylinders at the front face.

Tractor-Trailer Truck Configuration

Tests with a scale model of the truck were carried out in the boundary-layer tunnel with negligible blockage effect (blockage ratio = 1.2%). The trailer was provided with rotating cylinders at its top leading and trailing edges. The L/H ratio for the trailer was approximately 3.75, which suggested that rotation of the rear cylinder will have virtually no effect on the drag reduction. The wind-tunnel tests substantiated this observation. Figure 11 shows variation of C_D with the cylinder speed ratio U_c/U for three cases: cylinder with smooth surface, cylinder surface roughness of grade 80, and cylinder surface roughness of grade 40. In the absence of the momentum injection ($U_c/U = 0$), the truck drag coefficient is around 0.81 and reduces to 0.765 at $U_c/U = 2$ for the smooth cylinder case. The surface roughness of the cylinder improves the performance, further reducing C_D to around 0.73 at $U_c/U = 2.1$ for the roughness grade of 80. Increasing the surface roughness to 40 drops the minimum C_D to 0.7, a reduction of around 13%! Considering the fact that 1) around 70% of goods in North America are transported by trucks; 2) depending upon the speed, approximately 40–70% of the power is expended in overcoming the aerodynamic drag; and 3) on an average, a truck travels around 160,000 km/year; even 1% reduction in the drag coefficient can translate into a substantial saving in the fuel cost.

With the positive influence of the cylinder roughness on the momentum injection process and associated reduction in the drag, it seemed logical to introduce the momentum more directly. This was achieved by using a rotating cylinder with 1) helical grooves and 2) splines running parallel to its axis of rotation. Furthermore, as pointed out before, the rear cylinder contributed virtually nothing to the boundary-layer control, being submerged in the separated shear layer. This suggested a need for a newer model with freedom to locate the second cylinder at a desired location downstream. Hence a second model of the tractor-trailer configuration (also 1/12 scale) was constructed. It had a 45-ft trailer with a slightly

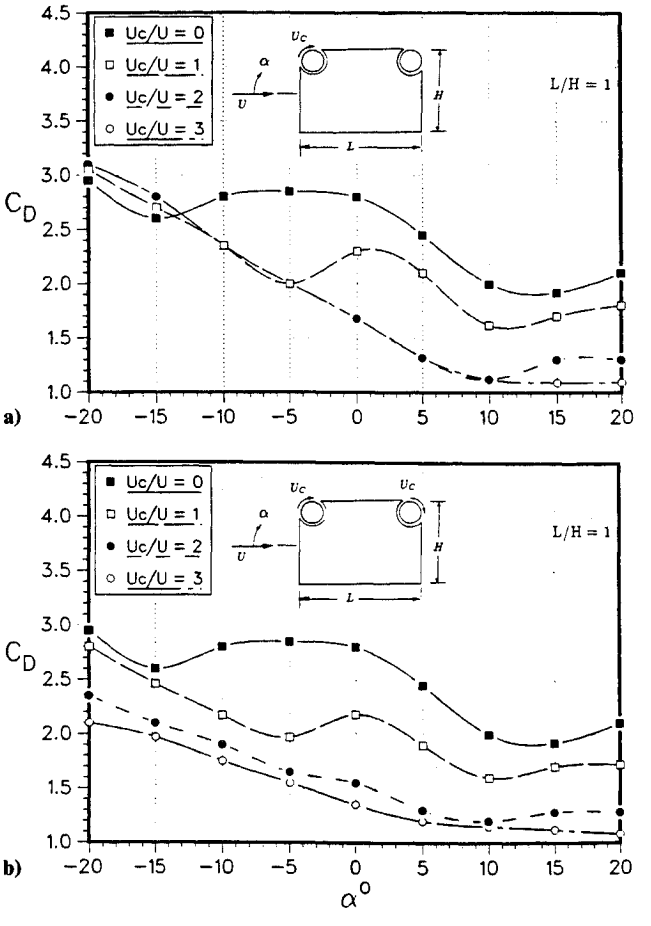

Fig. 9 Variation of the drag coefficient with the angle of attack for a two-dimensional square prism when the boundary-layer control is applied at the top surface: a) a rotating cylinder at the leading edge; b) rotating cylinders at leading and trailing edges.

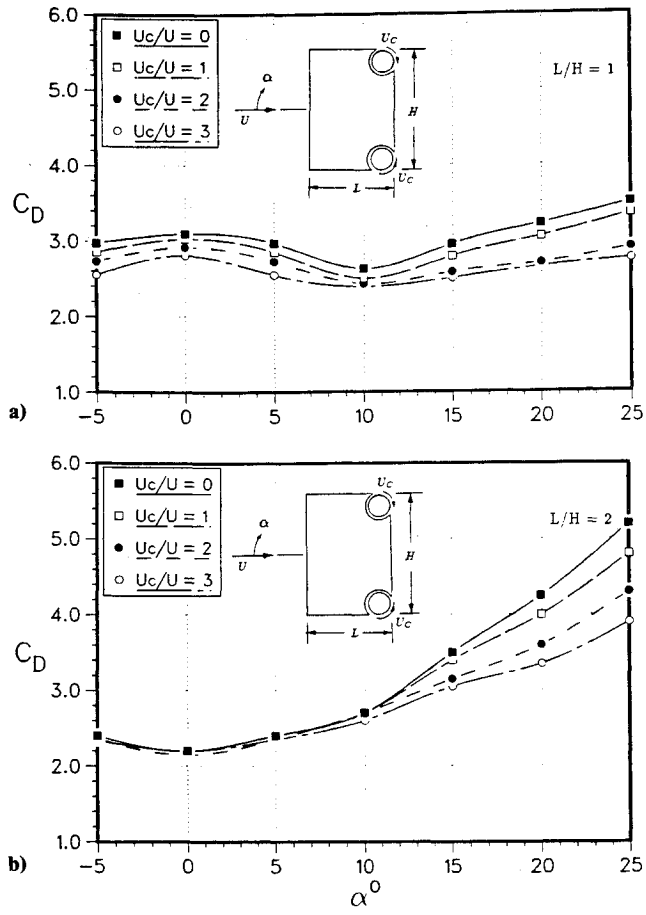

Fig. 10 Plots showing variation of the drag coefficient with the moving surface boundary layer control applied at the rear face of the prism: a) $L/H = 1$; b) $L/H = 2$.

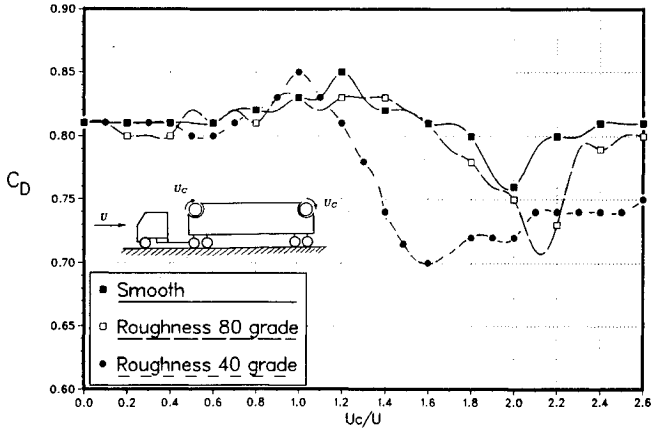

Fig. 11 Effect of the moving surface boundary-layer control on the drag coefficient of a tractor-trailer truck configuration.

different cab geometry and corresponded to one of the configurations selected for future road tests. In the present set of tests, the second cylinder was located 25.4 cm (10 in.) downstream of the leading edge cylinder.

Figure 12 shows the effect of the twin cylinders with helical grooves. At the outset it is apparent that the front cylinder rotation reduces the drag as before; however, character of the plot is rather different. There is a monotonic reduction in the drag coefficient with U_{cf}/U ($U_{cr}/U = 0$). Here U_{cf} and U_{cr} refer to the front and rear cylinders' surface speeds, respectively. Although the rear cylinder rotation further diminishes C_D, the reduction is relatively small. The maximum reduction in drag achieved was around 12.8%, about the same as the 40-grade surface roughness case studied before.

On the other hand, the spline cylinder reduces the drag coefficient dramatically (Fig. 13). To begin with, it should be recognized that the base drag coefficient of the truck with flush mounted spline cylinders in absence of rotation is higher than before (1.14 against 1.015 for the helical groove cylinders). Note, with only the front cylinder rotating ($U_{cf}/U = 6.1$), the drag coefficient reduces by about 29%. With the rear cylinder rotation, the drag reduction jumps to 41%. Even with the speed ratio of 4, the C_D reduced by around 22%. Thus the spline geometry appears quite promising in reducing pressure drag of the tractor- trailer truck configuration through MSBC.

In association with Canadian Pacific Transport Ltd., the largest truck company in Canada with an extensive network in North America, road tests are scheduled to begin in September 1991 using two distinctly different truck configurations. The tests will be conducted over the specified long-range route and at highway conditions with accurate monitoring of fuel consumption, mileage, wind speed and direction, load, etc. Such a fundamental study with bluff bodies complemented by flow visualization and field tests represents a useful step forward in assessing potential of the moving surface boundary-layer control concept.

A comment concerning practical application of the concept to real-life situations would be appropriate. High-speed rotation of the cylinders with an associated need for precise balancing to avoid vibration problems are logical concerns that would come to mind. As mentioned before, application of the concept to OV-10 aircraft[8,9] did not present any prob-

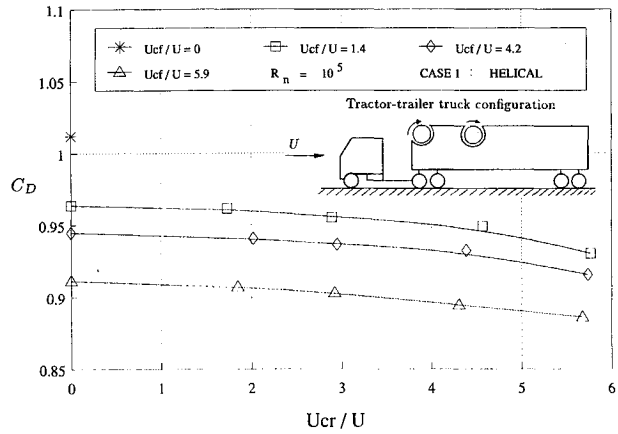

Fig. 12 Effect of momentum injection in the boundary layer using helical groove cylinders. The maximum drag reduction achieved was around 12.8%.

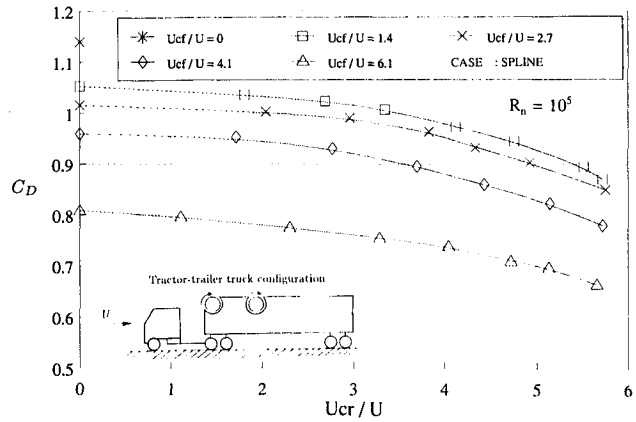

Fig. 13 Moving surface boundary-layer control on a truck model using twin spline cylinders. The drag reduction by 22% at $U_{cf}/U = U_{cr}/U = 4$ is indeed impressive.

lem. In the wind-tunnel experiments with conventional procedures for bearing alignment guaranteed smooth operation to cylinder rpm as high as 14,000.

Concluding Remarks

Based on a rather fundamental study of moving surface boundary-layer control with two-dimensional plates and prisms, as well as its application to a scale model of a typical tractor-trailer truck configuration, the following general conclusions can be made:

1) The concept appears to be quite promising in reducing drag of bluff bodies. For the flat plate at $\alpha = 90$ deg, it reduced the drag coefficient by 75%. The maximum reduction for a square prism varied from 54% ($L/H = 1$) to 40% ($L/H = 2$).

2) Effectiveness of the momentum-injecting device diminishes when located in the wake.

3) Surface roughness of the rotating cylinder tends to improve the boundary-layer control.

4) For a cylinder with the surface roughness of 40 grade, drag coefficient of the truck reduced by around 13% at $U_c/U = 1.5$. This promises to provide a significant reduction in the fuel cost.

5) A splined rotating cylinder injects momentum into the boundary-layer more directly presenting an exciting possibility of a further reduction in C_D.

6) The concept is essentially semipassive in character requiring negligible amount of power for its implementation.

Acknowledgments

The investigation reported here was supported by the Natural Sciences and Engineering Research Council of Canada, Grant A-2181 and Science Council of British Columbia, AGAR Grant SA-2. The models were fabricated in the Mechanical Engineering workshop. The assistance of E. Abell, Senior Technician, in construction of the model is gratefully acknowledged.

References

[1]Goldstein, S., *Modern Developments in Fluid Mechanics*, Vols. I and II, Oxford Univ. Press, London, 1938.

[2]Lachmann, G. V., *Boundary Layer and Flow Control*, Vols. I and II, Pergamon Press, Elmsford, NY, 1961.

[3]Rosenhead, L., *Laminar Boundary Layers*, Oxford Univ. Press, London, 1966.

[4]Schlichting, H., *Boundary Layer Theory*, McGraw-Hill, New York, 1968.

[5]Chang, P. K., *Separation of Flow*, Pergamon Press, Elmsford, NY, 1970.

[6]Favre, A., "Contribution a l'Etude Experimentale des Mouvements Hydrodynamiques a Deux Dimensions," Thesis, Univ. of Paris, Paris, 1938.

[7]Alvarez-Calderon, A., and Arnold, F. R., "A Study of the Aerodynamic Characteristics of a High Lift Device Based on Rotating Cylinder Flap," Stanford Univ., Stanford, CA, TR RCF-1, 1961.

[8]Cichy, D. R., Harris, J. W., and MacKay, J. K. "Flight Tests of a Rotating Cylinder Flap on a North American Rockwell YOV-10A Aircraft," NASA CR-2135, Nov. 1972.

[9]Weiberg, J. A., Giulianettij, D., Gambucci, B., and Innis, R. C., "Takeoff and Landing Performance and Noise Characteristics of a Deflected STOL Airplane with Interconnected Propellers and Rotating Cylinder Flaps," NASA TM X-62, 320, Dec. 1973.

[10]Cook, W. L., Mickey, D. M., and Quigley, H. G., "Aerodynamics of Jet Flap and Rotating Cylinder Flap STOL Concepts," AGARD Fluid Dynamics Panel on V/STOL Aerodynamics, Delft, The Netherlands, Paper 10, April 1974.

[11]Johnson, W. S., Tennant, J. S., and Stamps, R. E., "Leading Edge Rotating Cylinder for Boundary-Layer Control on Lifting Surfaces," *Journal of Hydrodynautics*, Vol. 9, No. 2, 1975, pp. 76–78.

[12]Modi, V. J., Sun, J. L. C., Akutsu, T., Lake, P., McMillian, K., Swinton, P. G., and Mullins, D., "Moving Surface Boundary Layer Control for Aircraft Operation at High Incidence," *Journal of Aircraft*, AIAA, Vol. 18, No. 11, 1981, pp. 963–968.

[13]Mokhtarian, F., and Modi, V. J., "Fluid Dynamics of Airfoils with Moving Surface Boundary Layer Control," *Proceedings of the AIAA Atmospheric Flight Mechanics Conference*, AIAA, New York, 1986; also *Journal of Aircraft*, Vol. 25, No. 2, Feb. 1988, pp. 163–169.